Materials Today Advances 7 (2020) 100099

Contents lists available at ScienceDirect

Materials Today Advances

journal homepage: www.journals.elsevier.com/materials-today-advances/

Metal oxides nanowires chemical/gas sensors: recent advances

E. Comini

Sensor, University of Brescia, Via Valotti 9, 25133, Italy

ARTICLE INFO

Article history:
Received 26 May 2020
Received in revised form
9 July 2020
Accepted 13 July 2020
Available online xxx

Keywords:
Chemical sensing
Gas sensing
Oxide semiconductors
Nanostructures
Functional materials

ABSTRACT

Chemical/gas sensors are playing and will play a crucial role in smart building, smart houses, environmental monitoring, food quality monitoring and in the customization of personalized medicine, as they allow a constant data collection to monitor all the parameters needed for a preventive intervention related to health and wealth of human beings together with the environment. Nanowires (NWs) and NW-based heterostructures thanks to their peculiar properties such as high crystallinity, flexibility, conductivity, and optical activity are key components of future sensing devices. Notwithstanding a rapid growth in smart, portable, and wearable chemical sensing devices, the development of reliable devices for the detection of chemicals, gases, and vapors is still needed together with the possibility to correlate the sensing data with health and wealth of the analyzed system: food, environment, and human beings. In this short review, I am going to report few recent studies and achievements devoted to increase the functional performances of chemical sensing devices, keeping the focus on materials, sensing transduction, and data extraction/evaluation.

© 2020 The Author. Published by Elsevier Ltd. This is an open access article under the CC BY-NC-ND license (http://creativecommons.org/licenses/by-nc-nd/4.0/).

1. Introduction

Nanomaterials have attracted the attention of researchers since long time ago, but among the different morphologies that can be found in literature, nanowires (NWs) related ones present the advantages of superior material quality together with an impressive design freedom. These are the characteristics that make NWs structures ready for pushing advancements in materials engineering and fundamental science. NWs represent a novel material category moving from conventional 2-dimensional films to 3-dimensional devices.

The ability to control material composition at a nanometric level is extremely relevant, especially for semiconducting materials. As different bandgap semiconductors are aligned, heterostructures (HSs) are formed and, due to the internal electric fields produced, carriers are displaced and localized [1].

In the specific case of NWs, there are several peculiarities and interesting possibilities that arise, as 3-dimensional HS can be prepared. Starting from a NW, a second nucleation can be achieved on the NW external surface resulting in hierarchical or branched HSs, increasing the surface-to-volume ratio that is critical for some applications such as catalysts, chemical, gas, or biosensors [2], and may be exploited also for electronic devices [3].

Moreover, lattice matching for having epitaxy is not a big constrain in NWs because the eventual strain can relax easily over an interface of few nanometers (as in the case of axial structures) [4]. Normally, the strain due to lattice mismatch combining two different constituents in NWs may relax elastically at the interface with no dislocations. Therefore, there is the capability to achieve HSs without looking for lattice matching, concentrating on the bandgap engineering [5–11]. In addition, in NW HSs, in the eventual case dislocations arise, they are misfit dislocations [12].

As we prepare HSs with NWs, the doping profile can be controlled on a 3-dimensional level; not only linear HSs but also radial ones can be easily achieved forming junctions [13–15].

In addition, NW HSs decoration with nanocluster or quantum dots is another frequently used possibility to change the material functional properties increasing specificities and tailoring real applications requirements [16].

All these capabilities to integrate different compounds, with no need of lattice

matching, may really be used for bandgaps engineering to achieve superior devices performances. Bandgap engineering is an essential property especially for semiconductors. Furthermore, the manifold possibilities and freedom in designing the shape and morphology allowed with NWs can open new and innovative material combinations and configurations.

When we are dealing with NWs, we can exploit also their exceptional flexibility. NWs can bear large mechanical

E-mail address: Elisabetta.comini@unibs.it.

https://doi.org/10.1016/j.mtadv.2020.100099
2590-0498/© 2020 The Author. Published by Elsevier Ltd. This is an open access article under the CC BY-NC-ND license (http://creativecommons.org/licenses/by-nc-nd/4.0/).

deformations without fracture or cracking, being so small they are incredibly robust and tough. Different and peculiar assemblies can be achieved on flexible substrates to develop high performances flexible, biocompatible, wearable sensors for the detection of chemical compounds, environmental air quality, human health, and food quality monitoring. Even the challenges related to massive integration nowadays are quite under control. The large aspect ratio together with the mechanical flexibility of NWs allow their processability through various techniques such as roll printing, drop casting, and spin coating [17–19].

In this short review, I will present few recent studies and achievements devolved to increase the functional performances of these devices, keeping the focus on materials, sensing transduction, and data extraction/evaluation as outlined in Fig. 1.

2. Growth of metal oxide chemical sensors

There are several possibilities to prepare NWs, but among them, 'bottom up' growth from the vapor phase is the most used even today after so many years of research in this area. It provides a high degree of crystallinity that is a key requirement for their successful integration in real devices. On the contrary 'top-down' growth may lead to surface defects, and it is generally costly and time-consuming, being therefore less efficient for the overall procedure.

The growth mechanism at the base of the majority of NW preparation experimental procedures is vapor-liquid-solid (VLS) as it may be exploited for a wide class of materials and structures [20–22].

There were some pioneering groups working on the preparation of NWs, demonstrating their superior performances with respect to their bulk counterpart [23–25]. Afterward, the materials community was focusing on their control in preparation and integration into new devices.

Different materials were synthesized such elemental semiconductors, II–VI and III–V semiconductors, nitrides, carbides, and oxides [26,27].

Oxides are a class of appealing materials because they can have interesting electrical properties spanning from insulator to quasi metallic behavior, high dielectric constants [28], wide bandgaps [29], and exceptional optical performances. Oxide materials have demonstrated their potentialities in solar cell, fuel cells, thermoelectric, photocatalysis, and sensors. Even sixty years after finding out for the first time the chemical/gas sensing properties of metal oxide semiconductors (MOXs) [30,31], this exceptional class of materials is still intensively investigated for chemical sensing. Moreover, with 1D nanostructures new possibilities in terms of devices and sensing mechanisms have been opened up. All these unique properties and possibilities still keep them among the key materials that will give rise to innovative devices with new functionalities and superior performances.

The growth capabilities, listed before, can be used to grow unique NWs and HSs on relatively inexpensive substrates, such as Si, quartz, polycrystalline alumina, or even plastic substrates for selected MOXs. Another peculiarity of these nanostructures is that NWs and HSs can easily form free-standing structures by detaching them from the substrate.

The biggest advantage of using VLS-based methods is the control of NW size, position, and dimensions; as a counterpart, the catalyst used to initiate the 1D growth normally remains at the top of the NWs.

For optical or photovoltaic applications, the presence of a metallic particle on the NWs tip may interfere with the device working principle, increasing electrical contact resistance, or increasing light reflection. However, in the case of chemical/gas sensors, this presence normally induces catalytic effects and therefore can be an advantage and may increase the sensing performances. Other problems with optoelectronic device performances are dislocations, formation of localized electronic states, recombination, trapping of carriers, depletion, and energy barriers formation. These phenomena are at the base of chemical sensing mechanism, therefore they do not necessary reduce the chemical sensing performances, even if they need to be controlled and reproduced in a reliable way for their real application as chemical/gas sensors.

Chemical sensors are devices that relate the presence of chemical compounds with a measurable signal, whose magnitude may be proportional to its concentration. The signal to be detected can be different: electrical resistance, conductance, capacitance, voltage, surface acoustic wave (SAW), magnetic, or optical characteristics. Among these, conductometric type remains the most studied also thanks to its cheap and reliable integration capabilities.

Conductometric MOX chemical sensors are well known since more than sixty years [29,30] as they provide several advantages, such as reduced costs and miniaturization compared with other

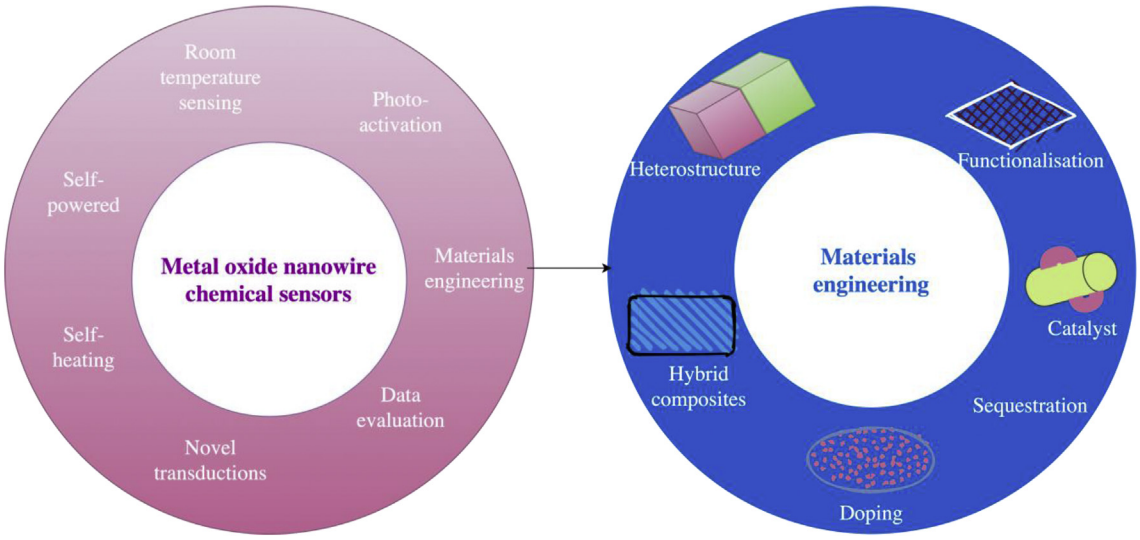

Fig. 1. Metal oxide nanowire chemical sensors and the strategies to increase their sensing performances.

sensing devices such as electrochemical or infrared sensors. Even though, they have several challenging points to tackle: selectivity, response/recovery times, sensitivity, and high operating temperatures [32,33]. Chemical sensing principle is based on MOX electrical resistance modulation by the surrounding atmosphere. Therefore, the active chemical sensing oxide is the key element affecting performance parameters such as sensitivity, selectivity, and response dynamics. The concentration information may be transduced in different ways. The interaction of the active material with the chemical compound may change its electrical characteristics, such as resistance or capacitance. In particular, MOX chemical sensors may have an electric, magnetic, or optical read out (based on their electrical, magnetic, or optical properties' modification). In MOXs, the conductance is determined by the surface reactions especially in presence of reactive species such as oxygen-inducing electron exchange between the chemisorbed species (O_2^- (ads), O^-(ads) and O^{2-}(ads)) and MOXs. To chemisorb, oxygen requires an activation energy; therefore each species is normally present in different temperature ranges. At temperatures lower than 400 °C, the predominant species present on the surfaces is O^-(ads). As oxygen molecules are chemisorbed, they extract electrons from the conduction band leading to the space-charge layer formation and to band bending. As a reducing compound interacts with the MOX surface, it may react with the adsorbed oxygen causing the release of trapped electrons back to the MOX conduction band and therefore increasing its conductance. These interactions may be reversible or irreversible, in the latter case causing a decrease of the response during the operation and in turn reducing its lifetime.

3. Enhancing the chemical sensing performances: active material

The oxide material preparation and post processing treatments will strongly influence sensitivity, selectivity, and response dynamics of the final device. Lately, many efforts were made in combining materials to form HSs, improving the sensing performances thanks to increased sites for absorption [34,35], enhanced catalytic activities [36,37], sequestration effect to increase selectivity [38,39]. MOX semiconductors may be n-type or p-type, whose majority charge carriers are electrons in the first case and holes in the latter, respectively. Conductometric chemical sensors are mostly made with n-type MOXs (SnO_2, WO_3, ZnO, TiO_2) as backbone with an n-type or p-type heterostructured material. N-type MOXs are normally preferred as backbones for HS formation because their response is proportional to the square of the one of p-type, and they are more stable [40]. In n-type MOXs, the absorbed oxygen ions form a depletion region close to the surface and charge carriers have to overcome the potential barrier at the boundaries. In p-type MOX, instead, a hole accumulation layer is formed decreasing their resistance [41]. It is this higher conductivity that decreases the possible variation of the carriers due to the adsorbed species. Nevertheless, the inclusion of p-type MOXs results in significant enhancements in chemical sensing performances thanks to their catalytic activity, p-n junction formation, increased surface reactivity, and adsorption sites. P-type MOXs show a high reactivity of lattice oxygen on the top of oxygen adsorbed from ambient atmosphere. Reports from catalyst research show that lattice oxygen is active in surface reactions following the Mars-van Krevelen mechanism [42–44]. The loss of oxygen can also be a possible cause for a decrease of the sensing performances during long-term operation of p-type MOXs. This reactivity significantly influences the chemical sensing performances. The challenge is finding models that can predict the sensing behavior because all these possible processes should be taken into account to get reliable predictions.

Recently, Raza et al. [45] reported on the chemical sensing performances of single crystal tin dioxide/polycrystalline nickel oxide core shell NWs structures. Thanks to atomic layer deposition, the nickel oxide shell thickness was varied between 2 and 8 nm. Nickel oxide shell deposition resulted in an electrical conductance decrease of several orders of magnitude, which was attributed to the Schottky barrier junctions across the n(core)-p(shell) interfaces. The hydrogen sensing performances were significantly depending on the NiO-shell layer thickness. The 4 nm NiO shell showed the best performances: almost four times higher than pristine SnO_2 NWs. This behavior was ascribed to NWs' high surface-to-volume ratio, nickel oxide conformality, and to the shell layer thickness optimization that in turn modulate the space-charge region.

Another strategy that was proposed in particular for hydrogen sulphide detection is the sulfurization of zinc oxide NWs [46]. This process resulted in a core shell NWs structure formation (zinc oxide core and zinc sulphide shell). These HSs proved a stable detection of H_2S. Moreover, Pd nanoparticles addition was used as a further activation procedure to improve the sensing performances together with a reduction in the operating temperature down to 200 °C. A relative variation of conductance of 4491% was registered in presence of 10 ppm of hydrogen sulphide with relatively fast response and recovery times together with a good selectivity to other toxic compounds. Furthermore, because the active material was deposited on a flexible substrate, the authors checked the variation of the response with substrate bending. The results proved stable chemical sensing performances even with 9 mm positive and 5 mm negative radius of curvature, experiments and numerical simulations showed a very good mechanical robustness (Fig. 2).

Addition of noble metals is a well known and studied strategy to tailor the chemical sensing performances, but lately also the incorporation of two catalyst have been proposed, and synergetic effects have been proven. Choi et al. [47] presented a codecoration with Pt and Pd on SnO_2, whereas Kim et al. [48] reported the effect of gold and palladium on WO_3. In both these works, the presence of the two catalysts enhances further the response. In the latter work, the formation of an alloy changes the electronic structure and, in turn, the sensor response toward acetone. The possibility of alloys or intermetallic compound formation is critical for chemical sensing and must be studied when choosing the components of the active material. The best way to exploit these synergetic effects is to prepare a HS that decreases the charge carrier concentration in the supporting material while increasing the surface reactivity in terms of reaction sites and rates. Unfortunately, when we deal with complex HSs, attention must be paid also to morphology, dispersion, potential interdiffusion at the interface and also to the thermal and exposure history. The properties of the interfaces between the HSs play an essential role in controlling the device functional properties. Sharp terminations and interruptions of the lattice translational symmetry will give rise to changes in the band structures, electrostatic potential discontinuity, and generate of a local electric field, which may present a barrier for charge transport.

Noble metal nanoparticles functionalization even though it is a well-established strategy to modulate the sensing performances is seldom studied in terms of optimization of the functionalization parameters. In a study by Lee et al. [49], SnO_2 NW functionalization with Pt and Pd was optimized in terms of chemical sensing performances toward nitrogen dioxide. The responses, reported as a function of the ratio between the surface area of the nanoparticles and the NW, result in a bell-shaped curve for both the catalysts. Moreover, the sensing mechanism was explained with a simple theoretical model based on the conduction channel modulation by chemical and electronic sensitization, providing some interesting guidance on the optimal catalyst coverage for the functionalization.

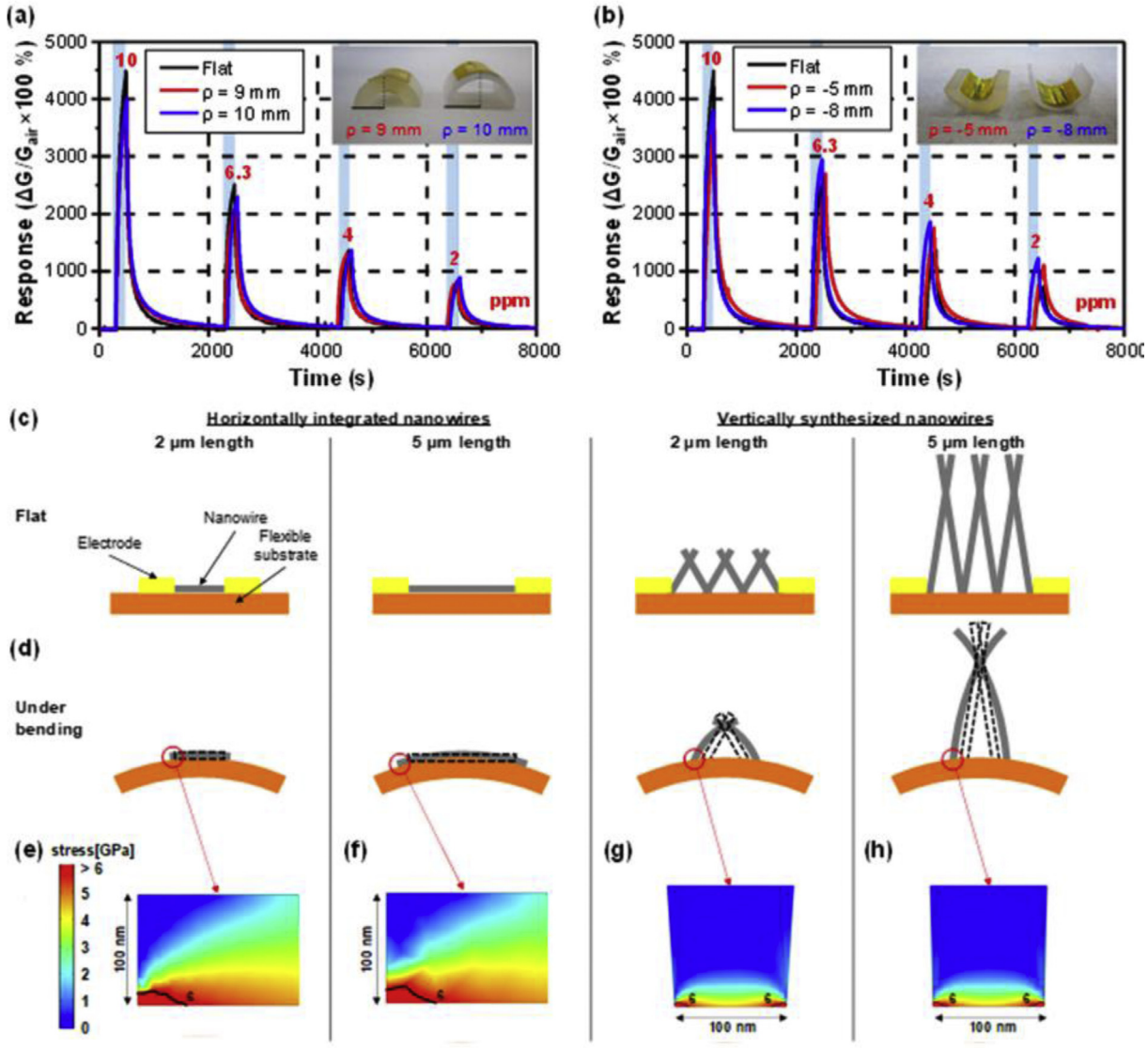

Fig. 2. Hydrogen sulfide (H_2S) gas sensing performance of palladium (Pd) nanoparticle–decorated zinc oxide/zinc sulfide (ZnO/ZnS) core-shell nanowires under bending conditions. Comparison of the sensing performances between (a) flat and positively bent surfaces (curvature radii: 9 and 10 mm) and (b) flat and negatively bent surfaces (curvature radii: −5 and −8 mm); schematic illustrations of deformation of horizontally integrated and vertically synthesized ZnO nanowires (c) in flat and (d) under the same bending conditions; stress profile at the edge of the horizontally integrated nanowire with (e) 2 and (f) 5 μm length and vertically synthesized nanowire with (g) 2 and (h) 5 μm length under 2% tensile loading. Reprinted with permission from a study by Yang et al. [46] Copyright 2019 American Chemical Society.

In addition to catalyzation, surface functionalization and HSs formation, doping has been effectively used to tune chemical sensing performances. An interesting work concerning doping effects on sensing was presented in 2020: alkaline-earth metals, including calcium, strontium, and barium, were introduced into the lattice of In_2O_3 nanotubes to finely tune the chemical selectivity [50]. This led to an improvement on formaldehyde sensing performances also compared with other chemical compounds. The 5% Ca-In_2O_3 chemical sensors exhibit a response of 116 to0wards 100 ppm formaldehyde which is about 4.5 and 10 times higher than those of ethanol and acetone at the same concentration, respectively. This enhancement was ascribed to the change in chemisorbed oxygen species, supported by X ray photoelectron spectroscopy (XPS) data, and the increase in basicity of the alkaline-earth.

Another way of doping is implantation. Implantation has not been extensively studied for MOX chemical sensor, also because it is a really expensive procedure. Recently, gas sensing performances improvements of SnO_2 NWs after Sb-ion implantation were presented [51]. Ions implantation was achieved with an ion implanter at 2×10^{13}–2×10^{15} ion/cm^2 doses. Nitrogen and sulfur dioxide chemical sensing performances were improved by antimony implantation especially for the lowest implantation dose tested. As the implantation dose increases further, the chemical sensing performances were decreasing. This behavior was attributed to a change of electron concentration by substituting Sn^{4+} ions to Sb^{+5} ions, and to surface defects creation.

Other than using noble metals as catalyst or doping strategies, the integration of organic materials with MOX in different forms has been proposed lately. Cellulose nanocrystals and apoferritin were incorporated into electrospinning solution to ease tungsten oxide nanotube synthesis, as a sensitization inducing $Na_2W_4O_{13}$ to achieve uniform functionalization with monodispersive apoferritin-derived platinum catalytic nanoparticles (2.22 ± 0.42 nm). This was resulting in highly selective hydrogen sulphide sensing performances with respect to other interfering

compounds. Furthermore, synergistic effects with a bioinspired Pt catalyst induced a remarkably enhanced H_2S response ($R_{air}/R_{gas} = 203.5$), with a very good selectivity ($R_{air}/R_{gas} < 1.3$ for the interferent gases) and rapid response (<10 s)/recovery (<30 s) time at 1 ppm of H_2S under 95% relative humidity level [52].

Unfortunately, despite all the reported efforts, developing material design strategies for MOXs to further enhance selectivity toward specific chemicals, especially when their activity is similar (e.g., acetone/benzene compounds), remains a difficult task. A synergic combination of metal-organic frameworks (MOFs) with MOX may play an important role in overcoming or mitigating this challenge. MOFs are types of microporous crystalline materials in which the pore structure may be controlled and used as a channel for selective separation of chemical compounds [53–56]. Many groups showed that this combination is a good strategy to combine MOX sensitivity to MOFs selectivity. The selectivity is greatly enhanced by modulating the channels in the MOF sheath thanks to the different kinetic diameters of chemical compounds with similar sensing activities. Au-ZnO@ZIF NW arrays were prepared and the pore size in the MOF sheath was modified: the molecules with different kinetic diameter were successfully 'filtered' enhancing selectivity. The achieved results showed a selective response to acetone in presence of benzene, keeping a high sensitivity (LOD < 0.1 ppb), fast response/recovery, and excellent long-term stability under various humidity (0–90 RH%) conditions [57].

3.1. Room temperature chemical sensing

Most of the MOXs work at temperatures higher than 200 °C. However, their capability to work at lower temperatures or even room temperature (RT) is necessary for their applications in explosive environments. Moreover, in the case of RT chemical sensors there is no need of a heater easing their integration and lowering significantly power consumption. However, the relatively low sensitivity, slow response, and recovery kinetics especially at RT still limit their real applications. Nevertheless, a lot of research activity has been done in this topic.

RT sensing has been proposed especially for nitrogen dioxide. A cactus-like Si/WO_3 NW composite structures were tested and the optimal operating temperature found was RT, exhibiting a good response to nitrogen dioxide, relatively good sensing repeatability, selectivity, and stability. The enhancement in RT sensing performances was attributed to efficient chemical sensitization and carrier modulation by a high-density p-n junction structure at the interface between the silicon NWs and tungsten oxide NWs [58].

Wang et al. [59] achieved a highly sensitive and fast response nitrogen dioxide RT sensor with a sulfonated reduced graphene oxide (S-rGO) functionalization of tungsten oxide nanorods. The MOX functionalization with S-rGO provides new capabilities for RT sensing. WO_3/S-rGO sensors response was 149% toward 20 ppm NO_2, proving an enhancement of 4.7 times and 100 times faster response compared WO_3/rGO sensors. Furthermore, the sensors exhibit good reproducibility, selectivity, and extremely fast recovery kinetics. In addition to the high transport capability of S-rGO and its excellent nitrogen dioxide adsorption ability, the WO_3/S-rGO enhancement in sensing performances was attributed to a favorable charge transfer at the HSs interface. A Schottky-type junction is formed at the WO_3/S-rGO interface, resulting in the upward band bending and a depletion region formation. This can act as a charge transport highway to induce the electron transfer to the electrodes together with excellent electrical conductivity of S-rGO.

Among the different strategies proposed to achieve RT sensing, photoactivation is one of the most studied. It consists in using light to activate the chemical interaction between MOX and target analytes. Moreover, when using UV light an additional effect is a cleaning process of MOX surface. In a study by Espid et al. [60], the effects of photoactivation on chemical sensing have been studied for ZnO nanoparticles and NWs. In the case of nanoparticles, the sensing response was 0.41–5 ppm NO_2, whereas it improved significantly to 1.5 by using photoactivation with 365 nm UV light and 25 mW/cm^2 power density. As far as ZnO NWs are concerned, a further enhancement of the sensing performances was registered, whereas 0.1 wt% platinum catalyzed ZnO NW sensors exhibited a response of 4.33–5 ppm NO_2 with a response time of 140s. This value is one order of magnitude higher and 50s faster than the response of zinc oxide nanoparticles. The improved performances were attributed to the role of platinum active sites in promoting NO_2 adsorption on zinc oxide NWs surface, as well as enhancing the layer electron utilization, together with the larger number of photogenerated electrons.

In addition to Pt, other metal nanoclusters were used as a way to increase the effect of photoactivation. The chemical sensing properties of ZnO nanorods catalyzed with gold nanoparticles were tested at RT with and without visible light activation and compared with pure ZnO [61]. The hybrid sensing element exhibited a visible light activity due to surface plasmon resonance effects of gold nanoparticles. The ZnO/Au sensors were more selective to ammonia in dark, while exhibited high selectivity to nitrogen dioxide with photoactivation, short response, and recovery time, as well as good reversibility at RT. The different selectivity was attributed to the opposite direction of electron transfer between ZnO and Au nanoparticles in dark and with photo activation, which changes the nanorods surface depletion characteristics. Furthermore, visible and UV photoactivation was reported as a way to enhance hydrogen sensing in tin dioxide NWs catalyzed with silver nanoparticles. The enhancement was ascribed to plasmonic hot electrons populating the silver nanoparticles surface [62].

In addition to nitrogen dioxide and hydrogen, also other chemical compounds were attracting the interest of researchers as acetone for example. WO_3 nanofibers photoactivated amperometric sensors were tested toward various concentrations of acetone, with different bias voltages in the range of 3–7 V. The maximum photoactivated response was 1.79 mA at 7 V for 12.5 ppm acetone at an optimal operating temperature of 350 °C. A 70 ppb detection limit was reported at a lower bias voltage with a repeatability of 99% [63].

UV activation is commonly more successful in enhancing the chemical sensing properties at relatively low temperatures, but few reports demonstrate that UV activation may be effective even at high temperatures [64]. Pt- or perovskite-decorated β-Ga_2O_3 nanorod arrays showed an UV-enhanced detection of CO at 500 °C. This effect was attributed to the increased population of photoinduced electron-hole pairs for Pt decorated ones. For perovskite-decorated nanorod arrays, the enhancement was attributed to a combination of the sensitizing effect and photocurrent effect.

4. Self-heating and self-powered devices

Self-heating was firstly proposed with thin films [65], but in this case, it was not energetically efficient. Several years after, with the advent of NWs, it was proposed in a single NW configuration [66]. This configuration requires an expensive preparation procedure in terms of time and costs. Nevertheless, few reports now have demonstrated the possible and efficient exploitation of self-heating in NW networks [67]. Self-heated SnO_2 NWs sensors were prepared by using UV lithography for the deposition of contacts and catalysts, controlling NW network and nanojunction density with the electrode gap size [68]. The chemical sensors prepared with a narrow gap resulted in a dense NW network, while a large gap resulted in a

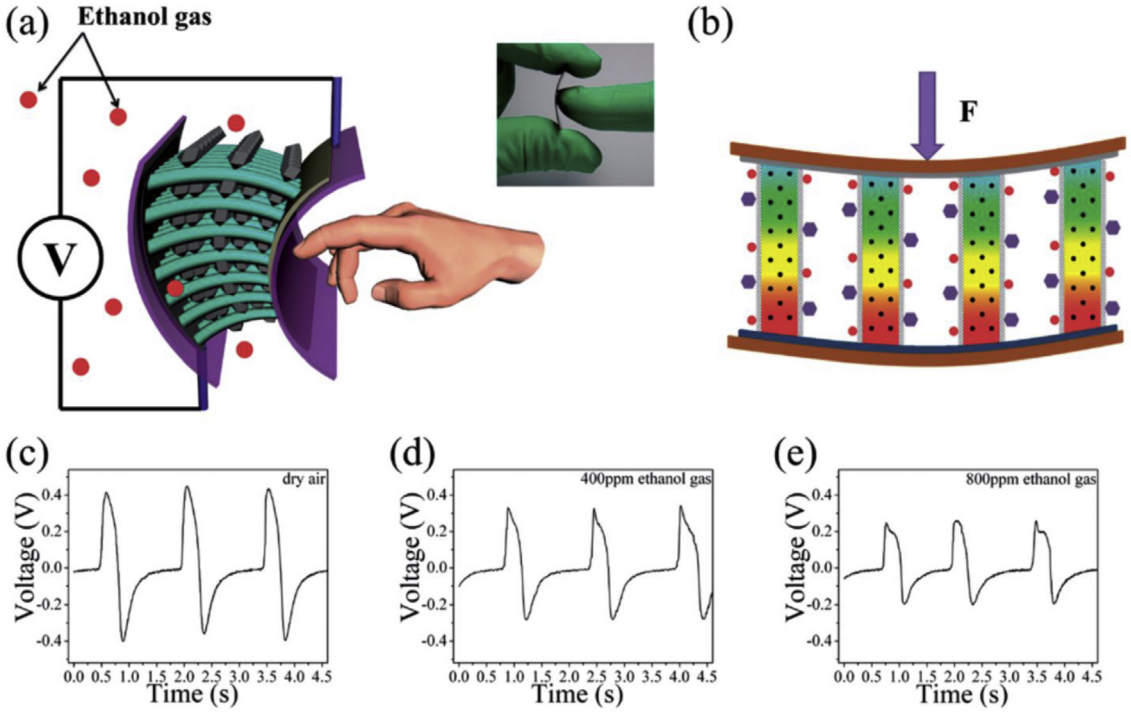

Fig. 3. (a) Schematic diagram showing that the flexible self-powered active ethanol sensor can be driven by human finger movement. (b) Schematic illustration of the piezoelectric output of the flexible device in ethanol gas. (c)–(e) are experimental piezoelectric outputs driven by human finger movement in air, 400 and 800 ppm ethanol gas, respectively. Used with permission of Royal Society of Chemistry, from the study 'Room-temperature self-powered ethanol sensing of a Pd/ZnO nanoarray nanogenerator driven by human finger movement' by Lin et al. [72] Nanoscale 6 (2014) 4604; Copyright 2014, permission conveyed through Copyright Clearance Center, Inc.

sparse network. A 20 μm electrode gap showed the best chemical sensing performances for C_2H_5OH with 4 mW power. The local nanojunction heating resulted more effective than network heating for self-heated NW sensors as far as power consumption and sensing performances are concerned.

Moreover, platinum and palladium functionalized ZnO NW selective toluene and benzene sensors in self-heating mode at RT were presented [69]. As 20 V voltage was applied, the maximum response of Pt-ZnO NWs was 2.86 toward 50 ppm of toluene. For Pd-ZnO NWs, instead, the maximum response was 2.20 toward 50 ppm of benzene. The enhancement of the chemical sensing properties was ascribed to the heterointerfaces creations.

Lately, Schottky-contact gas sensors were proposed in different applications, showing enhanced sensing performances especially in terms of dynamics [70]. The rapid response dynamics of the Schottky-contact devices was ascribed to the local contact. The width and height of the barrier vary as chemical absorption takes place: a high Schottky barrier height prevents the current from flowing, while a very low one will behave nearly as an ohmic-contact. Small changes of the Schottky barrier height significantly

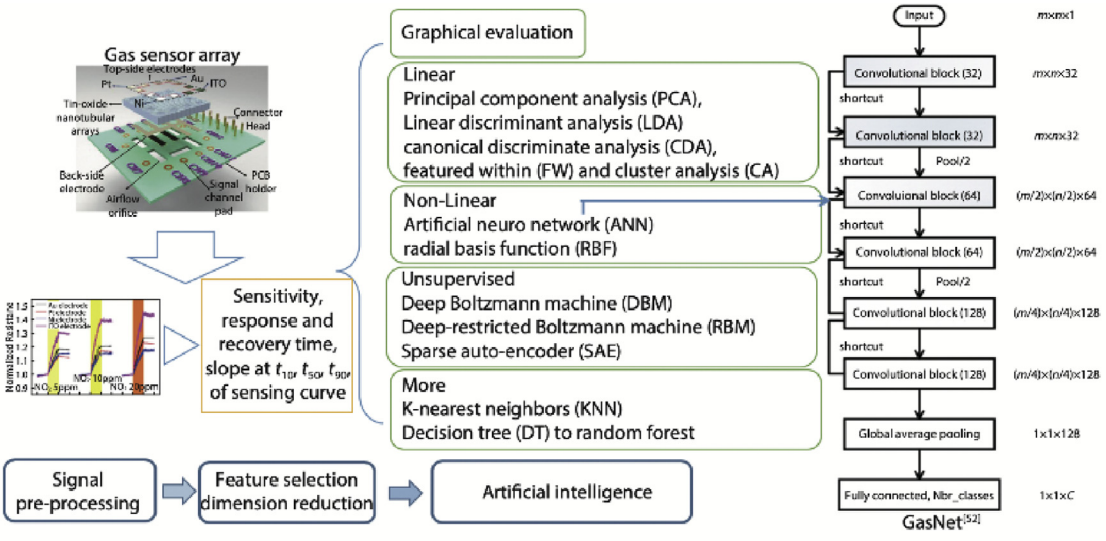

Fig. 4. Artificial intelligence algorithms adopted in a gas sensor array. Reprinted with Permissions from a study by Chen et al [78].

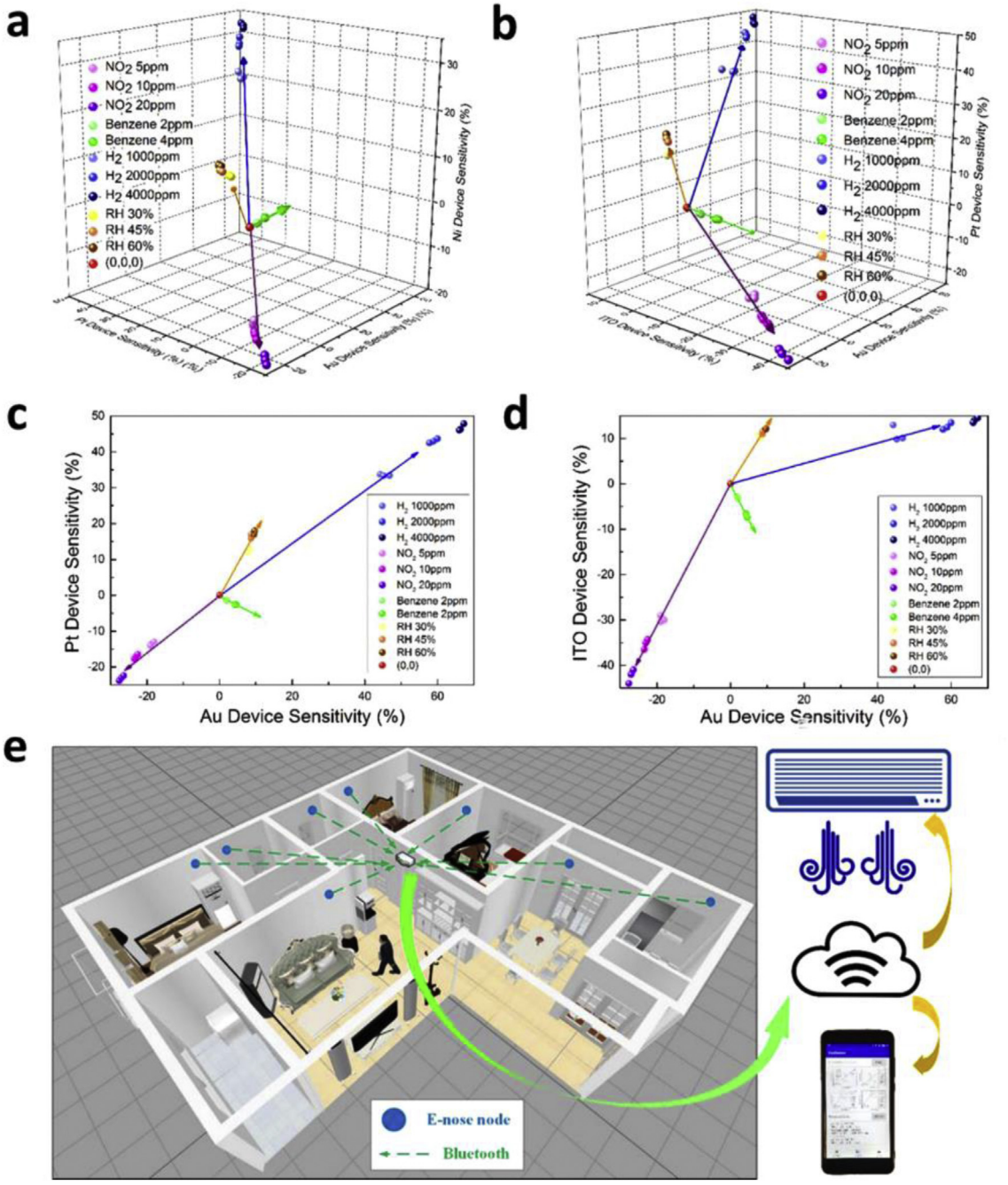

Fig. 5. Distinguishing ability of the E-nose and illustration of the E-nose in an indoor application. (a and b) LVQ method for gas classification in cubic maps. (c and d) Top views of corresponding cubic maps. (e) Illustration of the proposed E-nose application in future smart buildings. Reprinted with permission from a study by Chen et al. [80]. Copyright 2018 American Chemical Society.

change the device conductance with an exponential relationship. Further improvements were achieved with piezotronic effect. Indium/zinc oxide nanoarrays were integrated into self-powered gas sensor was designed by Zang et al. [71]. The presence of indium oxide was found to facilitate the charge transfer upon exposure to hydrogen sulphide increasing the response about seven times compared with ZnO NWs alone, while keeping a very good selectivity.

Moreover, in the same year a flexible self-powered ethanol sensor operating at RT was presented by Lin et al. [72]. The piezoelectric output of the Pd/ZnO NWs arrays was used as power source and RT ethanol sensor. When 800 ppm of ethanol was introduced, the piezoelectric output voltage decreased from 0.52 V (in air) to 0.25 V thanks to the catalytic effect of palladium, the Schottky barrier at the Pd/ZnO interface and ZnO NWs piezotronics effect. Moreover, this flexible ethanol sensor may be driven by mechanical energy such as with human finger movement (Fig. 3). Compared with conventional conductometric mode, the chemical/gas sensors based on piezoelectrical effect can work without external power source, reducing the energy consumption while requiring less effort for the final device development. The challenge is the need of a constant compressive force for the detection of the chemical

compound; therefore still some advancements are necessary before their use in practical applications.

5. SAW transductions mechanism

Another possibility for the exploitation of NWs in chemical/gas sensors is the development of SAW devices. These devices are characterized by their small size, low cost, good sensitivity, and capability of detecting a wide variety of compounds. SAW sensors register a change in the acoustic wave velocity or attenuation due to a change in the physical or chemical properties of the surface [73], and normally they rely on mass and/or conductance change of the active material. An interesting study reported ZnO NWs integration into SAW sensors by using gold catalyst and pulsed laser deposition technique [74]. Gold catalyst was patterned in order to study the influence on the geometric patterns on the sensing performances while keeping exposed areas and NWs morphology unchanged. The results showed that there is a strong dependence on the noise from the geometry of the active layer, while no significant change in the frequency shift. In particular, a configuration with longitudinal stripes has a noise signal 2.5 times smaller than the square zone. Moreover, a further increase in the noise was evident as ZnO film was deposited on the active area. This came together with an increasing frequency shift that was correlated with an increasing active surface.

6. Data evaluation

Last, but not least, I would also like to talk about the final part of the chemical sensor, that is, data evaluation. It is often treated as something independent form the device itself, while actually I feel that a great effort should be done to work synergistically, data analyses researchers together material scientists, in a holistic way. Even after several years of research on chemical/gas sensors, a quantitative detection in real environments with multiple chemical compounds and mixtures still remains challenging, especially for MOX chemical sensors due to intrinsic limitations arising from their working principle as described before. The main strategies to enhance the selectivity of MOX have already been presented from the material point of view, but in real situations a single chemical sensor is still not enough. Therefore, an array of chemical/gas sensors must be used to detect and analyze the volatile chemical compounds in real environments.

In this case, the challenge is moved from materials to data analyses. The data acquired from multiple chemical sensors have to be analyzed and normally a first investigation is made by a pattern-recognition method to distinguish the chemical compounds. From the first report of Persaud and Dodd [75] and Carpenter et al. [76] in 1982, significant achievements have been made also in this topic. Learning vector quantization, principal component analysis, partial least squares, multiple linear regression, principal component regression, and discrimination function analysis are the computational methodologies conventionally used for chemical sensors data analyses [77]. Pattern-recognition algorithms can be divided into several categories in accordance with certain standards as summarized in Fig. 4. The real challenge, as the detection of mixtures is concerned, is eventual non-linearity between responses and chemical concentrations together with the non-additive effect of the chemical interaction between the MOX surface and different chemical compounds.

In the past decade, multimodular sensing using a single sensor device was proposed [63]. Another interesting attempt was presented in a study by Tonezzer et al. [79]. An electronic nose was developed using a single tin dioxide NW applying a thermal gradient and combining its responses at five different temperatures. It was reported the ability of this platform to distinguish among acetone, ammonia, carbon monoxide, ethanol, hydrogen, nitrogen dioxide, and toluene. Applying machine learning algorithms to these thermal fingerprints, the system was able to recognize the gas in the chamber with a 94.3% accuracy and estimate its concentration with an average error of 24.5%.

Lately, an interesting report was published by Chen et al. [80]. An e-nose was prepared by the incorporation of four electrodes (Pt, Ni, Au, and ITO) into a single device (Fig. 5). The sensor platform was formed by: read-out system, wireless data transmission unit together with mobile phone receiver and a data processing application. The chemical/gas sensors were operating in conductometric mode, allowing the creation of a data base. The training vectors were defined by the input data points extracted. Each vector was representing a specific chemical compound with no overlap between the patterns of different chemical compounds. This platform was applied in practical demonstration for the detection of H_2, NO_2, benzene, and humidity, the power consumption was only 1% compared than commercial SnO_2 thin film gas sensor.

Park et al. [81] presented an energy-efficient multisensor system based on microelectromechanical devices with a suspended NW for hazardous gases detection. Its performances were optimized through a multimode structure and a learning-based pattern recognition algorithm to reduce dimensionality and neural networks for selectivity improvement. The deviations in sensing characteristics were calibrated through a proposed self-calibration zooming structure and a wireless multichannel gas-sensor system prototype was experimentally verified to achieve 2.6 times efficiency improvement.

Unfortunately, as we are increasing the multidimensional pattern information extracted from the output signals, there comes a time when the datasets become too complex for conventional data processing method therefore requiring a set of techniques to extract useful information from data sets [82].

7. Conclusions

This short review was presenting some capabilities of MOXs. As few of these oxides show simultaneous variation of different properties such as electrical or optical ones as a result of changes in the surrounding environment, this should be investigated more deeply. If we look at the electrical resistance, for example, its value is influenced by the interaction with light, the change in temperature, humidity, or atmosphere. Researchers tend to eliminate simultaneous variations to acquire a single stable signal that relates univocally to the target quantity to sense, but in such a way they are reducing MOX potentialities. This capability may lead to the extraction of multidimensional patterns from a single sensor. These characteristic signals can be correlated in multiple sensing modes for the realization an array of signals with a single device, moving the challenge from materials to data extraction and evaluation that is a research topic that is increasingly growing over the last years.

Chemical/gas sensors combined in arrays can be employed for the achievement of smart homes, buildings and cities, and with the advent of Internet of Things (IoT) even greater opportunities will be available especially with 5G networks. Using chemical sensors in smart phone may allow gas leakage detection, indoor air quality control, explosive detection, and environmental safety monitoring, but also food quality control at individual level in terms of checking eventual allergies or contaminations before eating any food [83]. Arrays of chemical sensors will be incorporated in refrigerators to detect spoilage of foodstuffs to allow intelligent food preservation and utilization. They will help also online control of processes such as refrigeration, pasteurization, and vacuum packages upon detecting in real-time eventual problems. Monitoring of the whole

process of aliments starting from their production to final storage is essential to ensure food quality and avoiding its waste. Moreover, chemical sensors arrays together with IoT may enhance safety and security of human beings and animals, detecting the presence of unpleasant, dangerous compounds, gas leakages inside a house or in the environment, notifying to human beings in close proximity at the earliest time. Drugs, explosives, or others illegal items can be detected in real time at the customs with chemical/gas sensors instead of dogs which may suffer from behavior variations [84]. Furthermore, large potentialities reside in disease diagnosis, but in this case a further challenge is the compliancy of strict medical regulations and the real tests availability in connection with medical institutes. However, for real commercial devices, the achievement of more in-depth and holistic studies is necessary, together with the detection mechanisms mastering for sensing performances improvement.

Declaration of competing interest

The authors declare that they have no known competing financial interests or personal relationships that could have appeared to influence the work reported in this article.

Acknowledgements

The author would like to sincerely thank all the members of SENSOR laboratory that are supporting the research on metal oxide chemical sensing and herself.

References

[1] H. Störmer, R. Dingle, A. Gossard, W. Wiegmann, M. Sturge, Two-dimensional electron gas at A semiconductor-semiconductor interface, Solid State Commun. 29 (1979) 705–709.
[2] K.A. Dick, K. Deppert, M.W. Larsson, T. Martensson, W. Seifert, L.R. Wallenberg, L. Samuelson, Synthesis of branched “nanotrees” by controlled seeding of multiple branching events, nat, Mater 3 (2004) 380–384.
[3] D.B. Suyatin, J. Sun, A. Fuhrer, D. Wallin, L.E. Fröberg, L.S. Karlsson, I. Maximov, L.R. Wallenberg, L. Samuelson, H.Q. Xu, Electrical properties of self-assembled branched InAs nanowire junctions, Nano Lett. 8 (2008) 1100–1104.
[4] F. Glas, Critical dimensions for the plastic relaxation of strained axial heterostructures, in: Free-standing Nanowires, Phys. Rev. B: Condens. Matter Mater. Phys., vol. 74, 2006, p. 121302, https://doi.org/10.1103/PhysRevB.74.121302.
[5] H. Ye, P. Lu, Z. Yu, Y. Song, D. Wang, S. Wang, Critical thickness and radius for axial heterostructure nanowires using finite-element method, Nano Lett. 9 (2009) 1921, https://doi.org/10.1021/nl900055x.
[6] A. Biermanns, S. Breuer, A. Trampert, A. Davydok, L. Geelhaar, U. Pietsch, Strain accommodation in Ga-assisted GaAs nanowires grown on silicon (111), Nanotechnology 23 (2012), https://doi.org/10.1088/0957-4484/23/30/3057035, 305703.
[7] S. Raychaudhuri, E.T. Yu, Critical dimensions in coherently strained coaxial nanowire heterostructures, J. Appl. Phys. 99 (2006), https://doi.org/10.1063/1.2202697, 114308.
[8] K.L. Kavanagh, Misfit dislocations in nanowire heterostructures, Semicond. Sci. Technol. 25 (2010), https://doi.org/10.1088/0268-1242/25/2/024006, 024006.
[9] T.E. Trammell, X. Zhang, Y. Li, L.-Q. Chen, E.C. Dickey, Equilibrium strain-energy analysis of coherently strained core–shell nanowires, J. Cryst. Growth 310 (2008) 3084, https://doi.org/10.1016/j.jcrysgro.2008.02.037.
[10] F. Glas, Critical dimensions for the plastic relaxation of strained axial heterostructures in free-standing nanowires, Phys. Rev. B 74 (2006), 121302(R).
[11] G.E. Cirlin, V.G. Dubrovskii, I.P. Soshnikov, N.V. Sibirev, Y.B. Samsonenko, A.D. Bouravleuv, J.C. Harmand, F. Glas, Critical diameters and temperature domains for MBE growth of III–V nanowires on lattice mismatched substrates, Phys. Status Solidi RRL 3 (2009) 112, https://doi.org/10.1002/pssr.200903057.
[12] M. De La Mata, C. Magen, P. Caroff, J. Arbiol, Atomic scale strain relaxation in axial semiconductor III-V nanowire hetero- structures, Nano Lett. 14 (2014) 6614–6620.
[13] K. Haraguchi, T. Katsuyama, K. Hiruma, K. Ogawa, GaAs p-n junction formed in quantum wire crystals, Appl. Phys. Lett. 60 (1992) 745–747.
[14] C. Colombo, D. Spirkoska, M. Frimmer, G. Abstreiter, A. Fontcubertal Morral, Ga-assisted catalyst-free growth mechanism of GaAs nanowires by molecular beam epitaxy, Phys. Rev. B Condens. Matter 77 (2008) 155326.
[15] B.M. Kayes, H.A. Atwater, N.S. Lewis, Comparison of the device physics principles of planar and radial p-n junction nanorod solar cells, J. Appl. Phys. 97 (2005) 114302.
[16] J. Arbiol, C. Magen, P. Becker, G. Jacopin, A. Chernikov, S. Schafer, F. Furtmayr, M. Tchernycheva, L. Rigutti, J. Teubert, S. Chatterjee, J.R. Morante, M. Eickhoff, Self-assembled GaN quantum wires on GaN/AlN nanowire templates, Nanoscale 4 (2012) 7517–7524.
[17] Q. Huang, Y. Zhu, Printing conductive nanomaterials for flexible and stretchable electronics: a review of materials, processes and applications advanced materials, Technologies 4 (2019) 1800546, https://doi.org/10.1002/admt.201800546.
[18] W. Xu, S. Zhang, W. Xu, Recent progress on electrohydrodynamic nanowire printing, Sci. China Mater 62 (2019) 1709–1726, https://doi.org/10.1007/s40843-019-9583-5.
[19] W. Gao, H. Ota, D. Kiriya, K. Takei, A. Javey, Flexible electronics toward wearable sensing ,acc, Chem. Res. 52 (2019) 523–533.
[20] E.I. Givargizov, Fundamental aspects of VLS growth, J. Cryst. Growth 31 (1975) 20–30.
[21] E.I. Givargizov, Highly Anisotropic Crystals, Reidel, 1987, p. 394.
[22] P. Yang, H. Yan, S. Mao, R. Russo, J. Johnson, R. Saykally, N. Morris, J. Pham, R. He, H.J. Choi, Controlled growth of ZnO nanowires and their optical properties, Adv. Funct. Mater. 12 (2002) 323.
[23] D. Li, Y. Wu, P. Kim, L. Shi, P. Yang, A. Majumdar, Thermal conductivity of individual silicon nanowires, Appl. Phys. Lett. 83 (2003) 2934–2936.
[24] A. Tao, F. Kim, C. Hess, J. Goldberger, R. He, Y. Sun, Y. Xia, P. Yang, Langmuir-blodgett silver nanowire monolayers for molecular sensing using surface-enhanced Raman spectroscopy, Nano Lett. 3 (2003) 1229–1233.
[25] E. Comini, G. Faglia, G. Sberveglieri, Z. Pan, Z.L. Wang, Stable and highly sensitive gas sensors based on semiconducting oxide nanobelts, Appl. Phys. Lett. 81 (2002) 1869, https://doi.org/10.1063/1.1504867.
[26] N. Wang, Y. Cai, R.Q. Zhang, Growth of nanowires, Mater. Sci. Eng. R Rep. 60 (2008) 1–51, https://doi.org/10.1016/j.mser.2008.01.001.
[27] M.H. Huang, Y. Wu, H. Feick, N. Tran, E. Weber, P. Yang, Catalytic growth of zinc oxide nanowires by vapor transport, adv, Mater 13 (2001) 113–116.
[28] J. Robertson, High dielectric constant gate oxides for metal oxide Si transistors, Rep. Prog. Phys. 69 (2006) 327.
[29] A.V. Emeline, G.V. Kataeva, A.V. Panasuk, V.K. Ryabchuk, N.V. Sheremetyeva, N. Serpone, Effect of surface photoreactions on the photocoloration of a wide band gap metal Oxide: probing whether surface reactions are photocatalytic, J. Phys. Chem. B 109 (2005) 5175–5185.
[30] A. Bielanski, J. Deren, J. Haber, Electric conductivity and catalytic activity of semiconducting oxide catalysts, Nature 179 (1957) 668–669, https://doi.org/10.1038/179668a0.
[31] T. Seiyama, A. Kato, K. Fujiishi, M. Nagatani, A new detector for gaseous components using semiconductive thin films,, Anal. Chem. 34 (1962), https://doi.org/10.1021/ac60191a001, 1502f.
[32] G.C. Korotcenkov, Engineering approaches for the improvement of conductometric gas sensor parameters, Sensor. Actuator. B Chem. 188 (2013) 709–728.
[33] G.C. Korotcenkov, Engineering approaches to improvement of conductometric gas sensor parameters: II. Decrease of dissipated (consumable) power and improvement stability and reliability, Sensor. Actuator. B Chem. 198 (2014) 316–341.
[34] H. Zhang, J. Feng, T. Fei, S. Liu, T. Zhang, SnO2 nanoparticles-reduced graphene oxide nanocomposites for NO2 sensing at low operating temperature, Sensor. Actuator. B Chem. 190 (2014) 472–478.
[35] L. Wang, et al., Designed synthesis of In2O3 Beads@TiO2-In2O3composite nanofibers for high performance NO2 sensor at room temperature, ACS Appl. Mater. Interfaces 7 (2015) 27152–27159.
[36] S. Park, G.J. Sun, C. Jin, H.W. Kim, S. Lee, C. Lee, Synergistic effects of a combination of Cr2O3-functionalization and UV-irradiation techniques on the ethanol gas sensing performance of ZnO nanorod gas sensors, ACS Appl. Mater. Interfaces 8 (2016) 2805–2811.
[37] J.H. Kim, et al., Highly selective and sensitive xylene sensors using Cr2O3-ZnCr2O4 hetero-nanostructures prepared by galvanic replacement, Sensor. Actuator. B Chem. 235 (2016) 498–506.
[38] H.R. Kim, A. Haensch, I.D. Kim, N. Barsan, U. Weimar, J.H. Lee, The role of NiO doping in reducing the impact of humidity on the performance of SnO2-based gas sensors: synthesis strategies, and phenomenological and spectroscopic studies, Adv. Funct. Mater. 21 (2011) 4456–4463.
[39] H.M. Jeong, J.H. Kim, S.Y. Jeong, C.H. Kwak, J.H. Lee, Co3O4-SnO2 hollow heteronanostructures: facile control of gas selectivity by compositional tuning of sensing materials via galvanic replacement, ACS Appl. Mater. Interfaces 8 (2016) 7877–7883.
[40] M. Hübner, C.E. Simion, A. Tomescu-StAnoiu, S. Pokhrel, N. Bârsan, U. Weimar, Influence of humidity on CO sensing with p-type CuO thick film gas sensors, Sens. Actuators, B 153 (2010) 347–353.
[41] H.-J. Kim, J.-H. Le, Highly sensitive and selective gas sensors using p-type oxide semiconductors: Overview, Sens. Actuators B: Chem 192 (2014) 607–627.
[42] J. Védrine, Heterogeneous catalysis on metal oxides, Catalysts 7 (2017) 341.
[43] X.Y. Liu, A. Wang, T. Zhang, C.Y. Mou, Catalysis by gold: new insights into the support effect, Nano Today 8 (2013) 403–416.
[44] M.J. Madou, S.R. Morrison, M.J. Madou, S.R. Morrison, 5 – catalysis background chemical sensing with solid state devices, (1989), 159–196.

[45] M.H. Raza, N. Kaur, E. Comini, N. Pinna, Toward optimized radial modulation of the space-charge region in one-dimensional SnO2−NiO Core−Shell nanowires for hydrogen sensing ACS appl, Mater. Interfaces 12 (2020) 4594−4606.
[46] D. Yang, I. Cho, D. Kim, M.A. Lim, Z. Li, J.G. Ok, M. Lee, I. Park, Gas sensor by direct growth and functionalization of metal oxide/metal sulfide core−shell nanowires on flexible substrates, ACS Appl. Mater. Interfaces 11 (2019) 24298−24307, https://doi.org/10.1021/acsami.9b06951.
[47] S.W. Choi, A. Katoch, G.J. Sun, S.S. Kim, Bimetallic Pd/Pt nanoparticle-functionalized SnO2nanowires for fast response and recovery to NO2, Sens, Actuators B Chem. 181 (2013) 446−453.
[48] S. Kim, S. Park, S. Park, C. Lee, Acetone sensing of Au and Pd-decorated WO3 nanorod sensors, Sens. Actuators, B 209 (2015) 180−185.
[49] J.-H. Lee, A. Mirzaei, J.-Y. Kim, J.-H. Kim, H.W. Kim, S.S. Kim, Optimization of the surface coverage of metal nanoparticles on nanowires T gas sensors to achieve the optimal sensing performance, Sensor. Actuator. B Chem. 302 (2020) 127196.
[50] Q. Liang, X. Zou, H. Chen, M. Fan, G-D. Li High-performance formaldehyde sensing realized by alkaline-earth metals T doped In2O3 nanotubes with optimized surface properties, Sensor. Actuator. B Chem. 304 (2020) 127241.
[51] J.-H. Kim, A. Mirzaei, J.-Y. Kim, J.-H. Lee, H.W. Kim, S. Hishita, S.S. Kim, Enhancement of gas sensing by implantation of Sb-ions in SnO2 nanowires, Sensor. Actuator. B Chem. 304 (2020) 127307.
[52] D.-H. Kim, J.-S. Jang, W.-T. Koo, S.-J. Choi, H.-J. Cho, M.-H. Kim, S.-J. Kim, I.-D. Kim, Bioinspired cocatalysts decorated WO3 nanotube toward unparalleled hydrogen sulfide chemiresistor, ACS Sens. 3 (2018) 1164−1173, https://doi.org/10.1021/acssensors.8b00210.
[53] C. Gu, N. Hosono, J.-J. Zheng, Y. Sato, S. Kusaka, S. Sakaki, S. Kitagawa, Design and control of gas diffusion process in a nanoporous soft crystal, Science 363 (2019) 387−391.
[54] H. Tian, H. Fan, M. Li, L. Ma, Zeolitic imidazolate framework coated ZnO nanorods as molecular sieving to improve selectivity of formaldehyde gas sensor, ACS Sens. 1 (2016) 243−250.
[55] K. Adil, Y. Belmabkhout, R.S. Pillai, A. Cadiau, P.M. Bhatt, A.H. Assen, G. Maurin, M. Eddaoudi, Gas/vapour separation using ultra-microporous metal−organic frameworks: insights into the structure/separation relationship, Chem. Soc. Rev. 46 (2017) 3402−3430.
[56] L. Li, R.-B. Lin, R. Krishna, H. Li, S. Xiang, H. Wu, J. Li, W. Zhou, B. Chen, Ethane/ethylene separation in a metal-organic framework with iron-peroxo sites, Science 362 (2018) 443−446.
[57] M.-S. Yao, L.-A. Cao, Y.-X. Tang, G.-E. Wang, R.-H. Liu, P. Naresh Kumar, G.-D. Wu, W.-H. Deng, W.-J. Hong, G. Xu, Gas transport regulation in a MO/MOF interface for enhanced selective gas detection, J. Mater. Chem. 7 (2019) 18397−18403.
[58] W. Zhang, M. Hu, X. Liu, Y. Wei, N. Li, Y. Qin, Synthesis of the cactus-like silicon nanowires/tungsten oxide nanowires composite for room-temperature NO_2 gas sensor, J. Alloys Compd. 679 (2016) 391−399.
[59] T. Wang, J. Hao, S. Zheng, Q. Sun, D. Zhang, Y. Wang, Highly sensitive and rapidly responding room-temperature NO2 gas sensors based on WO3 nanorods/sulfonated graphene nanocomposites, Nano Research 11 (2018) 791−803, https://doi.org/10.1007/s12274-017-1688-y.
[60] E. Espid, B. Adeli, F. Taghipour, Enhanced gas sensing performance of photo-activated, Pt-decorated, single-crystal ZnO nanowires, J Electrochemical Soc 166 (2019) H3223−H3230.
[61] J. Wang, S. Fan, Y. Xia, C. Yang, S. Komarneni, Room-temperature gas sensors based on ZnO nanorod/Au hybrids: visible- T light-modulated dual selectivity to NO2 and NH3, J. Hazard Mater. 381 (2020) 120919.
[62] N. Cattabiani, C. Baratto, D. Zappa, E. Comini, M. Donarelli, M. Ferroni, A. Ponzoni, G. Faglia, Tin oxide nanowires decorated with Ag nanoparticles for visible light-enhanced hydrogen sensing at room temperature: bridging conductometric gas sensing and plasmon-driven catalysis, J. Phys. Chem. C 122 (2018) 5026−5031.
[63] M. Imran, S. Sulthan, A. Abdul, H. Rashid, Y. Sabri, N. Motta, T. Tesfamichael, P. Sonar, M. Shafiei, Template based sintering of WO3 nanoparticles into porous tungsten oxide nanofibers for acetone sensing applications, J. Mater. Chem. C 7 (2019) 2961.
[64] H.-J. Lin, H. Gao, P.-X. Gao, UV-enhanced CO sensing using Ga_2O_3-based nanorod arrays at elevated temperature, Appl. Phys. Lett. 110 (2017) 43101.
[65] A. Salehi, A highly sensitive self heated SnO2 carbon monoxide sensor, Sens, Actuators B-Chem. 96 (2003) 88−93, https://doi.org/10.1016/S0925-4005(03)00490−00498.
[66] E. Strelcov, S. Dmitriev, B. Button, J. Cothren, V. Sysoev, A. Kolmakov, Evidence of the self-heating effect on surface reactivity and gas sensing of metal oxide nanowire chemiresistors, Nanotechnology 19 (2008), https://doi.org/10.1088/0957−4484/19/35/355502, 355502.
[67] N.D. Chinh, N.V. Toan, V.V. Quang, N.V. Duy, N.D. Hoa, N.V. Hieu, Comparative NO2 gas-sensing performance of the self-heated individual, multiple and networked SnO2 nanowire sensors fabricated by a simple process, Sens. Actuators B-Chem. 201 (2014) 7−12, https://doi.org/10.1016/j.snb.2014.04.095.
[68] T.M. Ngoc, N. Van Duy, N. Duc Hoa, C.M. Hung, H. Nguyen, N.V. Hieu, Effective design and fabrication of low-power-consumption self-heated SnO2 nanowire sensors for reducing gases, Sensor. Actuator. B Chem. 295 (2019) 144−152.
[69] J.-H. Kim, J.-H. Lee, Y. Park, J.-Y. Kim, A. Mirzaei, H. Woo Kim, S.S. Kim, Toluene- and benzene-selective gas sensors based on Pt- and Pd- T functionalized ZnO nanowires in self-heating mode, Sensor. Actuator. B Chem. 294 (2019) 78−88.
[70] C.F. Pan, R.M. Yu, S.M. Niu, G. Zhu, Z.L. Wang, Piezotronic effect on the sensitivity and signal level of Schottky contacted proactive micro/nanowire nanosensors, ACS Nano 7 (2013) 1803−1810.
[71] W. Zang, Y. Nie, D. Zhu, P. Deng, L. Xing, X. Xue, Core−shell In2O3/ZnO nanoarray nanogenerator as a self-powered active gas sensor with high H2S sensitivity and selectivity at room temperature, J. Phys. Chem. C 118 (2014) 9209−9216, https://doi.org/10.1021/jp500516t.
[72] Y. Lin, P. Deng, Y. Nie, Y. Hu, L. Xing, Y. Zhang, X. Xue, Room-temperature self-powered ethanol sensing of a Pd/ZnO nanoarray nanogenerator driven by human finger movement, Nanoscale 6 (2014) 4604.
[73] A.J. Ricco, S.J. Martin, T.E. Zipperian, Surface acoustic wave gas sensor based on film conductivity changes, Sens. Actuators, A 8 (1985) 319−333.
[74] A. Marcu, I. Nicolae, C. Viespe, Active surface geometrical control of noise in nanowire-SAW sensors, Sensors. Actuators B 231 (2016) 469−473.
[75] K. Persaud, G. Dodd, Analysis of discrimination mechanisms in the mammalian olfactory system using a model nose, Nature 299 (1982) 352, https://doi.org/10.1038/299352a0.
[76] M.A. Carpenter, S. Mathur, A. Kolmakov, Metal Oxide Nanomaterials for Chemical Sensors, Springer Science & Business Media, New York, NY, 2012.
[77] T.C. Pearce, S.S. Schiffman, H.T. Nagle, J.W. Gardner, Handbook of Machine Olfaction: Electronic Nose Technology, John Wiley & Sons, Hoboken, NJ, 2006.
[78] Z. Chen, Z. Chen, Z. Song, W. Ye, Z. Fan, Smart gas sensor arrays powered by artificial intelligence, J. Semiconduct. 40 (2019) 111601.
[79] M. Tonezzer, Selective gas sensor based on one single SnO2 nanowire, Sensors. Actuators: B. Chemical 288 (2019) 53−59.
[80] J. Chen, Z. Chen, F. Boussaid, D. Zhang, X. Pan, H. Zhao, A. Bermak, C.-Y. Tsui, X. Wang, Z. Fan, Ultra-low-power smart electronic nose system based on three-dimensional tin oxide nanotube Arrays, ACS Nano 12 (2018) 6079−6088, https://doi.org/10.1021/acsnano.8b02371.
[81] K. Park, S. Choi, H.Y. Chae, C.S. Park, S. Lee, Y. Lim, H. Shin, J.J. Kim, An energy-efficient multimode multichannel gas-sensor system with learning-based optimization and self-calibration schemes, IEEE Trans. Ind. Electron. 67 (2020) 3.
[82] I.A.T. Hashem, I. Yaqoob, N.B. Anuar, S. Mokhtar, A. Gani, S.U. Khan, The rise of “big data” on cloud computing: review and open research issues, Inf. Syst. 47 (2015) 98−115, https://doi.org/10.1016/j.is.2014.07.006.
[83] K. Chen, W. Gao, S. Emaminejad, Printed carbon nanotube electronics and sensor systems, Adv Mater 28 (2016) 4397.
[84] Snoopy Sniffer for concealed people discovery, Grant Agreement ID: 313110 1 January 2014-31 December 2016 Funded under: FP7-SECURITY.